

# Coupling of $\bar{K}^*N$ to the $\Lambda(1520)$

T. Hyodo<sup>1\*</sup>, Sourav Sarkar<sup>2†</sup>, A. Hosaka<sup>1</sup>, and E. Oset<sup>2</sup>

<sup>1</sup>*Research Center for Nuclear Physics, Ibaraki, Osaka 567-0047, Japan*

<sup>2</sup>*Departamento de Física Teórica and IFIC,*

*Centro Mixto Universidad de Valencia-CSIC,*

*Institutos de Investigación de Paterna, Aptd. 22085, 46071 Valencia, Spain*

## Abstract

We study the coupling of the  $\Lambda(1520) \equiv \Lambda^*$  resonance to the  $\bar{K}^*$  vector meson and nucleon. This coupling is not directly measured from the resonance decay, but is expected to be important in hyperon production reactions. We compute the coupling in two different schemes, one in the chiral unitary model where the  $\Lambda^*$  is dominated by the quasibound state of mesons and baryons, and the other in the quark model where the resonance is a  $p$ -wave excitation in the three valence quarks. It is found that there is a significant difference between the  $\Lambda^*\bar{K}^*N$  couplings in the two models. In the chiral unitary model  $|g_{\Lambda^*\bar{K}^*N}| \sim 1.5$ , while in the quark model  $|g_{\Lambda^*\bar{K}^*N}| \sim 10$ . The difference of the results stems from the different structure of the  $\Lambda^*$  in both models, and hence, an experimental determination of this coupling would shed light on the nature of the resonance.

## 1 Introduction

Recent activities in hadron physics have been stimulated by the discussions on exotic states. The existence of the exotic pentaquark  $\Theta^+$  [1] is not yet confirmed, but much of the works are related to explain its expectedly unusual properties. Exotic states, by definition, contain more than three quarks in the case of baryons, and more than one quark-antiquark pair in the case of mesons. In both cases, the exotic states may have components of two or more color singlet states. If the color-singlet correlations such as  $[\bar{q}q]_{\text{singlet}}$  and  $[qqq]_{\text{singlet}}$  are strong, the states may be regarded as composite states of two or more hadrons. However, if the color-nonsinglet correlations such as diquark correlations are strong, the components of color singlet states are only a small part of the exotic states.

Such color-singlet or color-nonsinglet correlations may be tested not only in the manifestly exotic states but also in ordinary hadrons. The role of diquark correlations in

---

\*Present address: Yukawa Institute for Theoretical Physics, Kyoto University, Kyoto 606-8502, Japan

†Present address: Variable Energy Cyclotron Centre, 1/AF Bidhannagar, Kolkata-700064, India

hadrons has been discussed [2]. Contrary, the importance of color-singlet correlations may be tested by the mesonic cloud around baryons. The strong correlation between mesons and baryons, as implied by chiral perturbation theory, has been shown to generate baryon resonances especially in  $s$ -wave scattering channels: For instance, the  $\Lambda(1405)$  resonance which can be generated in  $s$ -wave  $\bar{K}N$  scattering [3, 4].

Recently, another  $\Lambda$  resonance, the  $\Lambda(1520) \equiv \Lambda^*$  of  $J^P = 3/2^-$ , has been investigated in several contexts. In Refs. [5, 6], the resonance was described as a quasibound state of  $\pi\Sigma(1385)$  and  $K\Xi(1530)$  in  $s$  wave. In these studies, the identification of some baryon resonances with  $s$ -wave quasibound state of an octet meson and a decuplet baryon has been extensively studied. This approach is further extended in particular to the  $\Lambda^*$ , by including the  $d$ -wave channels of mesons and ground state baryons [7, 8], leading to a successful description of existing data.

The  $\Lambda^*\bar{K}^*N$  coupling is worth being studied. In the experimental data [9] and its analysis for  $\Lambda^*$  photoproduction [10], the important role of  $\bar{K}^*$  vector meson was suggested, while a similar behavior was recently explained by means of the photo- $K^*$  contact term [11].

Here we investigate exclusively the  $\bar{K}^*$  coupling to the  $\Lambda^*$ , where the  $\Lambda^*$  is formed dominantly by the  $s$ -wave  $\pi\Sigma(1385)$  quasibound state, which is supplemented by the  $K\Xi(1530)$  state and the  $d$ -wave  $\bar{K}N$  and  $\pi\Sigma$  states. The result is compared with that of the conventional quark model, where the  $\Lambda^*$  is described as a  $p$ -wave excitation of one of the three valence quarks. This comparison should be useful in testing the very different nature of the two descriptions. For more detail of the computation, see Ref. [12].

## 2 Formulation

We consider an effective interaction Lagrangian [11] given by

$$\mathcal{L}_{\Lambda^*\bar{K}^*N} = \frac{g_{\Lambda^*\bar{K}^*N}}{M_{K^*}} \bar{\Lambda}^*_\mu \gamma_\nu (\partial^\mu K^{*\nu} - \partial^\nu K^{*\mu}) N + \text{h.c.} , \quad (1)$$

where  $M_{K^*}$  is the mass of the vector  $K^*$  meson, h.c. denotes the hermitian conjugate, and  $g_{\Lambda^*\bar{K}^*N}$  is the coupling constant. Because  $J^P(\Lambda^*) = 3/2^-$ , the coupling has two independent components. In terms of multipoles, they are  $E1$  and  $M2$ . Here, we investigate the  $s$ -wave coupling which is the  $E1$  amplitude in the chiral unitary model. We expect that the  $s$ -wave coupling dominates in the small three-momentum  $|\mathbf{k}|$  region, where  $\mathbf{k}$  is the relative momentum of the (virtual)  $\bar{K}^*$  and  $N$ . Assuming the interaction region of about 1 fm, the  $d$ -wave and hence the  $M2$  component will become important for  $|\mathbf{k}| > 400$  MeV.

Applying the nonrelativistic reduction to Eq. (1), and picking up the  $s$ -wave component, we obtain the transition amplitude of  $\bar{K}^*N \rightarrow \Lambda^*$  as

$$-it_{\Lambda^*\bar{K}^*N} = g_{\Lambda^*\bar{K}^*N} \mathbf{S}^\dagger \cdot \boldsymbol{\epsilon} . \quad (2)$$

Here  $\boldsymbol{\epsilon}$  is the polarization vector of the  $\bar{K}^*$  and  $\mathbf{S}$  is the spin transition operator.

In the chiral unitary model, the  $\Lambda^*$  is generated dynamically in the scattering of the  $\pi\Sigma^*$  and  $K\Xi^*$  channels in  $s$  wave and the  $\bar{K}N$  and  $\pi\Sigma$  channels in  $d$  wave [7, 8]. In order to estimate the coupling of the  $\Lambda^*$  resonance to the  $\bar{K}^*N$  channel, we follow the microscopic mechanism as illustrated in the left panel of Fig. 1. In this case, the  $\bar{K}^*N$  couples to the dynamically generated  $\Lambda^*$ , represented by the amplitude  $T$  in the figure, decaying into the  $\pi\Sigma^*$  channel. Notice that the  $K\Xi^*$  channel does not appear in the first

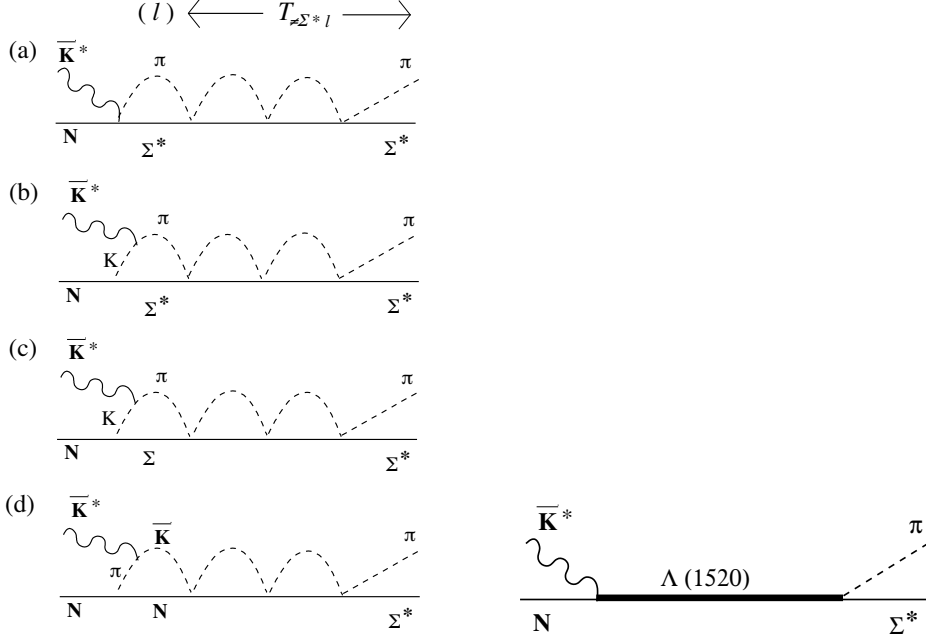


Fig. 1: Left: Diagrams for the microscopic mechanism of  $\bar{K}^*N \rightarrow \Lambda^* \rightarrow \pi\Sigma^*$  calculated in the chiral unitary model. Right: Diagram for the resonance dominance model of  $\bar{K}^*N \rightarrow \Lambda^* \rightarrow \pi\Sigma^*$ .

intermediate loop, since there is no direct coupling from  $\bar{K}^*N$  to  $K\Sigma^*$ . Schematically, the process  $\bar{K}^*N \rightarrow \Lambda^* \rightarrow \pi\Sigma(1385)$  can be expressed as

$$-it_{\text{ChU}} = \sum_l (-iT_{\pi\Sigma^*l}) iG_l (-it_{l\bar{K}^*N}),$$

where  $T_{\pi\Sigma^*l}$  is  $l \rightarrow \pi\Sigma^*$  amplitude obtained by the chiral unitary model [7, 8],  $G_l$  is the loop function of the intermediate state  $l$ , and  $-it_{l\bar{K}^*N}$  is the amplitude of  $\bar{K}^*N \rightarrow l$ .

Since we consider the  $s$ -wave coupling, the amplitude  $-it_{l\bar{K}^*N}$  should be written as  $-it_{l\bar{K}^*N} = g_{l\bar{K}^*N} \mathbf{S}^\dagger \cdot \boldsymbol{\epsilon}$ . Denoting the total energy as  $\sqrt{s}$ , we consider the energy region close to the  $\Lambda^*$  pole  $\sqrt{s} \sim M_{\Lambda^*}$ . In this region, the chiral unitary amplitude  $T_{ij}$  can be approximated by the Breit-Wigner propagator  $T_{ij} \sim g_{\Lambda^*i} g_{\Lambda^*j} / (\sqrt{s} - M_{\Lambda^*})$  with coupling constants  $g_{\Lambda^*i}$ , where  $i$  stands for the channels coupling to  $\Lambda^*$ . Then we have

$$-it_{\text{ChU}} \sim -ig_{\Lambda^*\pi\Sigma^*} \frac{i}{\sqrt{s} - M_{\Lambda^*}} \sum_l g_{\Lambda^*l} G_l g_{l\bar{K}^*N} \mathbf{S}^\dagger \cdot \boldsymbol{\epsilon}. \quad (3)$$

On the other hand, with the  $s$ -wave coupling Eq. (2), the resonance model for the amplitude  $\bar{K}^*N \rightarrow \Lambda^* \rightarrow \pi\Sigma(1385)$  can be written as shown in the right panel of Fig. 1,

$$-it_{\text{res}} = -ig_{\Lambda^*\pi\Sigma^*} \frac{i}{\sqrt{s} - M_{\Lambda^*}} g_{\Lambda^*\bar{K}^*N} \mathbf{S}^\dagger \cdot \boldsymbol{\epsilon},$$

where  $g_{\Lambda^*\bar{K}^*N}$  is the  $\Lambda^*\bar{K}^*N$  coupling constant that we are interested in. Hence comparing this amplitude with Eq. (3), we extract the  $\Lambda^*\bar{K}^*N$  coupling as

$$g_{\Lambda^*\bar{K}^*N} = \sum_l g_{\Lambda^*l} G_l g_{l\bar{K}^*N}. \quad (4)$$

In the previous study [8], the coupling constants  $g_{\Lambda^*l}$  have been determined as  $g_{\Lambda^*\pi\Sigma^*} = 0.91$ ,  $g_{\Lambda^*\pi\Sigma} = -0.45$ , and  $g_{\Lambda^*\bar{K}N} = -0.54$ , which well reproduce the partial decay widths. The contributions from (a)-(d) are given by [12]

$$\begin{aligned} -it^{(a)} - it^{(b)} &= (-iT_{\pi\Sigma^*\pi\Sigma^*})i \left( G_{\pi\Sigma^*} + \frac{2}{3}\tilde{G}_{\pi\Sigma^*K} \right) g_{\pi\Sigma^*\bar{K}^*N} \mathbf{S}^\dagger \cdot \boldsymbol{\epsilon} . \\ -it^{(c)} &= (-iT_{\pi\Sigma^*\pi\Sigma})i\tilde{G}_{\pi\Sigma K} g_{\pi\Sigma\bar{K}^*N} \mathbf{S}^\dagger \cdot \boldsymbol{\epsilon} , \\ -it^{(d)} &= (-iT_{\pi\Sigma^*\bar{K}N})i\tilde{G}_{\bar{K}N\pi} g_{\bar{K}N\bar{K}^*N} \mathbf{S}^\dagger \cdot \boldsymbol{\epsilon} , \end{aligned}$$

where  $G_{\pi\Sigma^*}$  and  $\tilde{G}_{\pi\Sigma^*K}$  are the loop functions

$$\begin{aligned} G_{\pi\Sigma^*}(\sqrt{s}) &= i \int \frac{d^4q}{(2\pi)^4} \frac{1}{q^2 - m_\pi^2 + i\epsilon} \frac{1}{\sqrt{s} - q^0 - E_{\Sigma^*} + i\epsilon} , \\ \tilde{G}_{\pi\Sigma^*K}(\sqrt{s}, k) &= i \int \frac{d^4q}{(2\pi)^4} \frac{\mathbf{q}^2}{(q-k)^2 - m_K^2 + i\epsilon} \frac{1}{q^2 - m_\pi^2 + i\epsilon} \frac{1}{\sqrt{s} - q^0 - E_{\Sigma^*} + i\epsilon} , \\ \tilde{G}_{\bar{K}N\pi}(\sqrt{s}, k) &= i \int \frac{d^4q}{(2\pi)^4} \frac{\mathbf{q}^2}{(q-k)^2 - m_\pi^2 + i\epsilon} \frac{\mathbf{q}^2}{q_{\text{on}}^2} \frac{1}{q^2 - m_K^2 + i\epsilon} \frac{M_N}{E_N} \frac{1}{\sqrt{s} - q^0 - E_N + i\epsilon} , \end{aligned}$$

with  $E_{\Sigma^*}(\mathbf{q}) = \sqrt{M_{\Sigma^*}^2 + \mathbf{q}^2}$  and the coupling constants are given by

$$g_{\pi\Sigma^*\bar{K}^*N} = \frac{1}{2}g \frac{g_A^*}{2f} , \quad g_{\bar{K}N\bar{K}^*N} = \sqrt{3}g \frac{D+F}{2f} , \quad g_{\pi\Sigma\bar{K}^*N} = \sqrt{2}g \frac{D-F}{2f} ,$$

We thus obtain the coupling of the  $\Lambda(1520)$  with  $\bar{K}^*N$  as

$$\begin{aligned} g_{\Lambda^*\bar{K}^*N}(\sqrt{s}, k) &= g_{\Lambda^*\pi\Sigma^*} \left[ G_{\pi\Sigma^*}(\sqrt{s}) + \frac{2}{3}\tilde{G}_{\pi\Sigma^*K}(\sqrt{s}, k) \right] g_{\pi\Sigma^*\bar{K}^*N} + g_{\Lambda^*\pi\Sigma} \tilde{G}_{\pi\Sigma K}(\sqrt{s}, k) g_{\pi\Sigma\bar{K}^*N} \\ &\quad + g_{\Lambda^*\bar{K}N} \tilde{G}_{\bar{K}N\pi}(\sqrt{s}, k) g_{\bar{K}N\bar{K}^*N} . \end{aligned} \quad (5)$$

### 3 Numerical results

Before calculating Eq. (5), let us consider the momentum variables. Since Eq. (3) is valid close to the pole of the resonance, we choose  $\sqrt{s} = 1520$  MeV. For this  $\sqrt{s}$ ,  $\Lambda^*$  cannot decay into  $\bar{K}^*(892)$  and  $N(940)$ . Here we assume that the  $\bar{K}^*$  is off the mass shell with the nucleon being on-shell. Then the energy of the  $\bar{K}^*$  can be given by

$$k^0 = \sqrt{s} - E_N(\mathbf{k}) = \sqrt{s} - \sqrt{M_N^2 + \mathbf{k}^2} ,$$

where we are in the center of mass frame. In order to study the finite momentum effect and stability of the result, we vary the momentum  $|\mathbf{k}|$  from zero to 400 MeV, and plot the real and imaginary parts as well as the absolute value of the  $\Lambda^*\bar{K}^*N$  coupling constant in the left panel of Fig. 2. We observe that the result is stable against the momentum  $|\mathbf{k}|$  up to  $\sim 200$  MeV, where the  $s$ -wave coupling is expected to be dominant. Numerical values are

$$g_{\Lambda^*\bar{K}^*N} \sim 1.53 + 0.41i, \quad |g_{\Lambda^*\bar{K}^*N}| \sim 1.58.$$

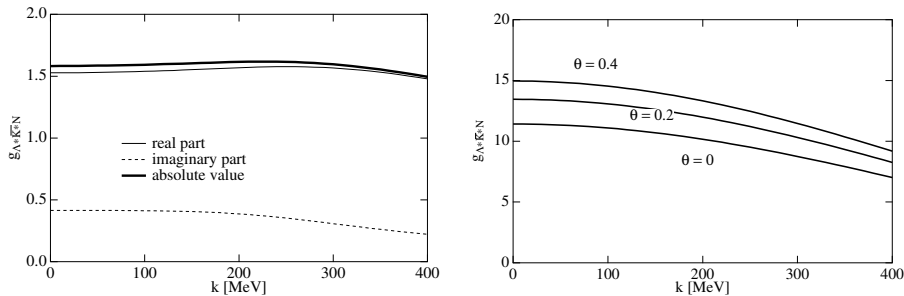


Fig. 2: Left: Numerical results for the  $\Lambda^* \bar{K}^* N$  coupling constant as a function of  $K^*$  momentum  $|\mathbf{k}|$  in the chiral unitary model. Thick solid line, thin solid line, and dashed line represent absolute value, real part, and imaginary part of the coupling constant, respectively. Right: Result in the quark model, for different mixing angles  $\theta$ .

The complex phase is the relative one to  $g_{\Lambda^* \bar{K} N} = -0.45$ .

In the quark model,  $\Lambda(1520)$  resonance is a  $p$ -wave state of 70-dimensional representation of  $SU(6)$  [13]. In the spin-flavor group, it is a superposition of  ${}^2\mathbf{1}$ ,  ${}^2\mathbf{8}$ , and  ${}^4\mathbf{8}$ . In the standard quark model,  $\Lambda^*$  is dominated by the flavor singlet  ${}^2\mathbf{1}$  with some mixture of  ${}^2\mathbf{8}$ ; the spin quartet  ${}^4\mathbf{8}$  has only a small fraction. Such a wave function has been tested for the decay of  $\Lambda^* \rightarrow \bar{K} N, \pi \Sigma$ , and has been proven to work reasonably well [13, 14]. The  $\Lambda^* \bar{K}^* N$  coupling constant is then related to the  $E1$  multipole amplitude by an overall constant  $g_{\Lambda^* \bar{K} N} = \frac{3}{\sqrt{6}} E1$ . In the calculation, we consider a mixing of  ${}^2\mathbf{1}$  and  ${}^2\mathbf{8}$  states for  $\Lambda(1520)$  as  $|\Lambda(1520)\rangle = \cos\theta|{}^2\mathbf{1}\rangle + \sin\theta|{}^2\mathbf{8}\rangle$ . In the Isgur-Karl model, the mixing angle was obtained  $\theta \sim 0.4$  [13]. The result is shown in the right panel of Fig. 2. The quark model value, in contrast with that of the chiral unitary approach, is of order  $g_{\Lambda^* \bar{K}^* N} \sim 10$ . In particular, the value increases slightly as the mixing angle increases, which is a consequence of the interference between the two flavor states. The difference between the values of the chiral unitary model and the quark model is large, and it would be interesting to test the coupling by experiments. In reality, the physical resonance state may be a mixture of the two extreme schemes of the chiral unitary and the quark models. The coupling  $g_{\Lambda^* \bar{K}^* N}$  could be used to investigate such a hybrid nature of the resonance.

## 4 Summary

We have studied the  $\Lambda(1520) \bar{K}^* N$  coupling constant. The motivations are twofold: One is to offer a model estimation for the unknown coupling constant which is expected to be important in hyperon production reactions, and the other one is to test different types of models for baryon resonances. In the chiral unitary model the resonances are described as a meson baryon quasibound state which may indicate the importance of hadron-like correlations in hadron structure. The resulting coupling constant  $g_{\Lambda^* \bar{K}^* N}$  is expressed as a sum over contributions from various channels necessary for the formation of  $\Lambda^*$ . The actual number of the coupling  $g_{\Lambda^* \bar{K}^* N}$  turned out to be of order 1-2, which is significantly smaller than the quark model value of order 10.

The difference in the results in two models should be a consequence of the difference of the model setup in various aspects. First, the quark model describes the  $\Lambda^*$  as a three-quark system, while it is five-quark description in the chiral unitary model. Second, in the

chiral unitary model, the  $\Lambda^*$  is mainly a member of flavor **8**, while in the quark model it is presumably dominated by the flavor singlet **1**. Third, the wave function of the  $\Lambda^*$  would be dominated by the  $s$ -wave component of  $\pi\Sigma(1385)$ , while it is a  $p$ -wave excitation in the quark model. Such differences in the internal structure should be reflected in the  $\Lambda^* \bar{K}^* N$  coupling. If the actual  $\Lambda(1520)$  has a mixed structure of the hadronic quasibound state and the three-quark state, the relevant coupling constant will be an intermediate value.

Since we have no experimental information of the coupling it would be very interesting to have the experimental value. Information from experiments as well as theoretical comparison would provide further understanding of the resonance structure.

T.H. thanks to the Japan Society for the Promotion of Science (JSPS) for support. S.S. wishes to acknowledge support from the Ministerio de Educacion y Ciencia in the program Doctores y Tecnologos extranjeros. This work is supported in part by the Grant for Scientific Research [(C) No.17959600, T.H.] and [(C) No.16540252, A.H.] from the Ministry of Education, Culture, Science and Technology, Japan and by the contract BFM2003-00856 from MEC (Spain) and FEDER, the Generalitat Valenciana and the E.U. EURIDICE network contract HPRN-CT-2002-00311. This research is part of the EU Integrated Infrastructure Initiative Hadron Physics Project under contract number RII3-CT-2004-506078.

## References

- [1] LEPS, T. Nakano *et al.*, Phys. Rev. Lett. **91**, 012002 (2003).
- [2] R. L. Jaffe, Phys. Rept. **409**, 1 (2005).
- [3] N. Kaiser, P. B. Siegel, and W. Weise, Nucl. Phys. **A594**, 325 (1995).
- [4] E. Oset and A. Ramos, Nucl. Phys. **A635**, 99 (1998).
- [5] E. E. Kolomeitsev and M. F. M. Lutz, Phys. Lett. **B585**, 243 (2004).
- [6] S. Sarkar, E. Oset, and M. J. Vicente Vacas, Nucl. Phys. **A750**, 294 (2005).
- [7] S. Sarkar, E. Oset, and M. J. Vicente Vacas, Phys. Rev. **C72**, 015206 (2005).
- [8] L. Roca, S. Sarkar, V. K. Magas and E. Oset, Phys. Rev. **C73**, 045208 (2006).
- [9] D. P. Barber *et al.*, Zeit. Phys. **C7**, 17 (1980).
- [10] A. Sibirtsev, *et al.*, hep-ph/0509145.
- [11] S.-I. Nam, A. Hosaka, and H.-C. Kim, Phys. Rev. **71**, 114012 (2005).
- [12] T. Hyodo, S. Sarkar, A. Hosaka, and E. Oset, Phys. Rev. **C73**, 035209 (2006).
- [13] N. Isgur and G. Karl, Phys. Rev. **D18**, 4187 (1978).
- [14] A. J. G. Hey, P. J. Litchfield, and R. J. Cashmore, Nucl. Phys. **B95**, 516 (1975).